2014 IEEE/RSJ International Conference on
Intelligent Robots and Systems (IROS 2014)
September 14-18, 2014, Chicago, IL, USA

# Towards Local Reflexive Control of a Powered Transfemoral Prosthesis for Robust Amputee Push and Trip Recovery

Nitish Thatte[1] and Hartmut Geyer[2]

***Abstract*— Transfemoral amputees often suffer from falls and a fear of falling that leads to a decreased quality of life. Existing control strategies for powered knee-ankle prostheses demonstrate only limited ability to react to disturbances that induce falls such as trips, slips, and obstacles. In contrast, prior work on neuromuscular modeling of human locomotion suggests that control strategies based on local reflexes exhibit robustness to unobserved terrain such as slopes and steps. Therefore, we propose that a powered knee-ankle prosthesis governed by reflexive local controls will more competently adapt to unperceived disturbances. To test this hypothesis, we simulate a neuromuscular model of a transfemoral amputee walking over rough ground with a powered knee-ankle prosthesis governed by the proposed reflexive controller. We show that the proposed control allows the amputee to walk farther over rough ground than does the state-of-the-art control. The proposed controller also more readily rejects deviations from nominal walking gaits such as those encountered during a trip. These results suggest that applying the proposed control to a powered knee-ankle prosthesis will substantially improve amputee gait stability.**

## I. INTRODUCTION

There are currently an estimated six hundred thousand lower limb amputees in the United States, a number expected to rise in the coming decades due to a growing diabetes epidemic [1]. These amputees often suffer from falls that result in injuries and a fear of falling that can lead to avoidance of activity and a decreased quality of life [2]. Transfemoral amputees are especially affected by this issue due to poor prosthesis controls that lead to reduced balance, compensatory movements, and unnatural gaits [3], [4].

To assist transfemoral amputees, manufacturers have released a number of prosthetic devices such as the Otto-bock C-leg and the Ossur Rheo Knee [5]. These devices employ microprocessor-controlled dampers that improve gait characteristics over uncontrolled prostheses. However, due to their use of mechanically passive components, these products cannot match human performance as they cannot perform positive net work over a gait cycle. Consequently, transfemoral amputees wearing these prostheses may suffer from increased energy consumption, slower ambulation speeds, and an inability to respond to unexpected disturbances such as trips, slips and pushes [6], [7].

To solve the kinematic, energetic, and robustness problems caused by mechanical-passivity, researchers have designed and tested powered knee-ankle prostheses. A notable example is Vanderbilt University's powered lower limb prosthesis [8]–[10]. This prosthesis uses impedance function control to drive its knee and ankle actuators. This strategy uses piecewise impedance functions to approximate the torque versus joint angle relationships for each phase of a healthy human gait cycle. With this control method, Sup et al. produced joint angles and torques for the knee and ankle similar to those seen during normal walking [10]. However, experiments also show that the required impedance functions vary greatly with the environment [11] and that impedance control must be augmented with a separate stumble classifier and recovery controller in order to respond to disturbances [12].

In contrast, ankle prostheses controlled by neuromuscular models have shown appropriate adaptations to sloped environments while also mimicking the kinematics and kinetics of healthy gait [13]. The neuromuscular models employed by these prostheses simulate muscles and local feedback reflexes to reproduce the joint torques seen during walking.

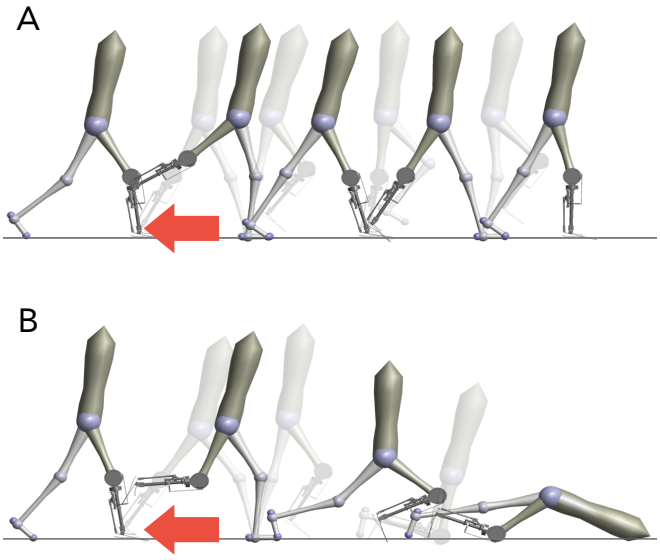


Fig. 1: Snapshots following a simulated tripping event. Response of the proposed local reflexive prosthetic control (A) and impedance control (B) to a 20 N-s impulse applied shortly after toe-off (red arrow). Local reflexive control successfully responds to the trip and continues walking. Impedance control cannot effectively react to the same disturbance and subsequently falls.

*This work was supported by the National Science Foundation and The Robotics Institute, Carnegie Mellon University.

[1]Nitish Thatte, nitisht@andrew.cmu.edu, and [2]Hartmut Geyer, hgeyer@cs.cmu.edu, are with The Robotics Institute, Carnegie Mellon University, 5000 Forbes Ave, Pittsburgh, PA 15213.

In this paper we present three contributions: First, we adapt a neuromuscular model in order to represent the anatomy and physiology of a transfemoral amputee (subsection III-A). Second, we present a preliminary mechatronic design for a powered knee-ankle prosthesis (subsection III-B). Last, we modify the neuromuscular model to obtain a prosthesis control based on muscle reflexes and local feedbacks (subsection III-C). To evaluate our proposed control, we simulate the coupled amputee-prosthesis system and perform optimizations to obtain model and control parameters that lead to robust locomotion over rough terrain (subsection IV-A). Finally, we compare the performance of the proposed local and reflexive controller to that of state-of-the-art impedance controller (subsection IV-C, subsection IV-D). Our results suggest that the proposed control may be more robust to elevation changes and unexpected deviations from nominal walking, as shown in Figure 1, and therefore may help prevent trips and falls.

## II. Review of Reflexive Walking Control

Neuromuscular models simulate the musculoskeletal system and hypothesised neural feedbacks. Previous work has shown that these models produce gaits that are kinetically, kinematically, and electromyographically similar to observed human locomotion patterns and that these models are robust to environmental changes such as elevation variations [14].

Specifically, here we review a neuromuscular model with robust foot placement control [15]. This model represents the musculoskeletal system with seven segments that comprise the torso and two three-segment legs. We connect these segments via six revolute joints that act as the hips, knees, and ankles. To actuate the joints, the model simulates seven Hill-type muscles [16] per leg: the soleus, gastrocnemius, tibialis anterior, vastus, hamstrings, hip flexors, and gluteus. When stimulated, these muscles produce torques

$$\tau_i^m = F^m(S,l,v)r^m(\phi_i) \tag{1}$$

about the joints, where $r^m(\phi_i)$ is the variable moment arm of muscle $m$ about joint $i$ and $F^m(S,l,v)$ is the force produced by the Hill-type muscle-tendon unit given a stimulation $S$, length $l$, and extension rate $v$.

### A. Neuromuscular Stance Control

During the gait cycle, the muscles of the stance leg are stimulated by reflexes primarily in the form of length and/or force feedbacks. In general,

$$S^m(t) = S_0^m + \sum_n G_n^m P_n^m(t-\Delta t_n^m) \tag{2}$$

where $S_0^m$ is muscle $m$'s constant prestimulation, $P_n^m(t-\Delta t_n^m)$ is the time-delayed proprioceptive length or force signal from muscle $n$ acting on muscle $m$, and $G_n^m$ is the gain on that signal. For more information about the specifics of the muscle and reflex pathway models, see [14], [15].

### B. Swing Leg Placement Control

During swing, a leg placement strategy prescribes desired foot placement locations, thereby increasing the model's robustness to trips, slips, and elevation changes. To obtain desired foot placement locations we use a feedback law,

$$\alpha_{tgt} = \alpha_0 + c_d d + d_v v, \tag{3}$$

taken from the SIMBICON control strategy [17]. In this control law, $\alpha_{tgt}$ is the target leg angle, $\alpha_0$ is the default leg angle, $d$ is the horizontal distance between the stance ankle and the center of mass, $v$ is the velocity of the center of mass, and $c_d$ and $c_v$ are constants.

The swing leg local control, described in full in [18], is inspired by hypothesized reflexes in biological legged systems. The knee control uses a finite state machine to switch between three phases outlined here. In the following equations, $\alpha$ is the angle of the leg, defined as the angle between horizontal and a line connecting the ankle and the hip, where negative $\dot{\alpha}$ indicates forwards swing of the leg, and $\phi_k$ is the knee angle, where negative $\dot{\phi}_k$ indicates knee flexion.

i The first phase allows the knee to passively flex in response to hip moments generated at the onset of swing

$$\tau_k^i = \begin{cases} 0, & \dot{\alpha} > 0 \\ k^i\dot{\alpha}, & \dot{\alpha} \le 0 \end{cases}. \tag{4}$$

If the leg angle decreases during this phase, the second case is active and applies a flexion torque to the knee in proportion to the leg angle speed, $\dot{\alpha}$, with a constant gain of $k^i$.

ii The second phase activates when the leg length contracts beyond a threshold,

$$\tau_k^{ii} = \begin{cases} -k_1^{ii}\dot{\phi}_k, & \dot{\phi}_k \le 0 \\ -k_2^{ii}\dot{\phi}_k(\alpha-\alpha_{tgt})(\dot{\phi}_k+\dot{\alpha}), & \dot{\phi}_k > 0 \ \&\ \dot{\phi}_k > -\dot{\alpha} \\ 0, & \text{otherwise} \end{cases}, \tag{5}$$

where $\alpha_{tgt}$ is the target knee angle from Equation 3, and $k_1^{ii}$ and $k_2^{ii}$ are damping coefficients. The first case dampens knee flexion. The second case dampens knee extension, but allows progressively more extension as the leg angle approaches its target. The $\dot{\phi}_k + \dot{\alpha}$ term prevents premature landing of the leg by damping the knee if it extends faster than the overall leg angle.

iii Finally, the third phase engages when the leg angle gets within a threshold of the target leg angle. In this phase, the controller applies torque to stop and extend the knee,

$$\tau_k^{iii} = \begin{cases} -k^{iii}(\alpha_{thr}-\alpha)\left(1-\frac{\dot{\alpha}}{\dot{\alpha}_{max}}\right), & \alpha < \alpha_{thr} \\ 0, & \dot{\alpha} < \dot{\alpha}_{max}, \text{ otherwise} \end{cases} \tag{6}$$

where $\dot{\alpha}_{max}$ is the maximum leg retraction velocity for which the stopping knee torque is applied. When this torque brings the leg velocity to zero, an additional knee extension torque is added,

$$\tau_k^{iii'} = \tau_k^{iii} + k^{ext}(l_0 - l), \tag{7}$$

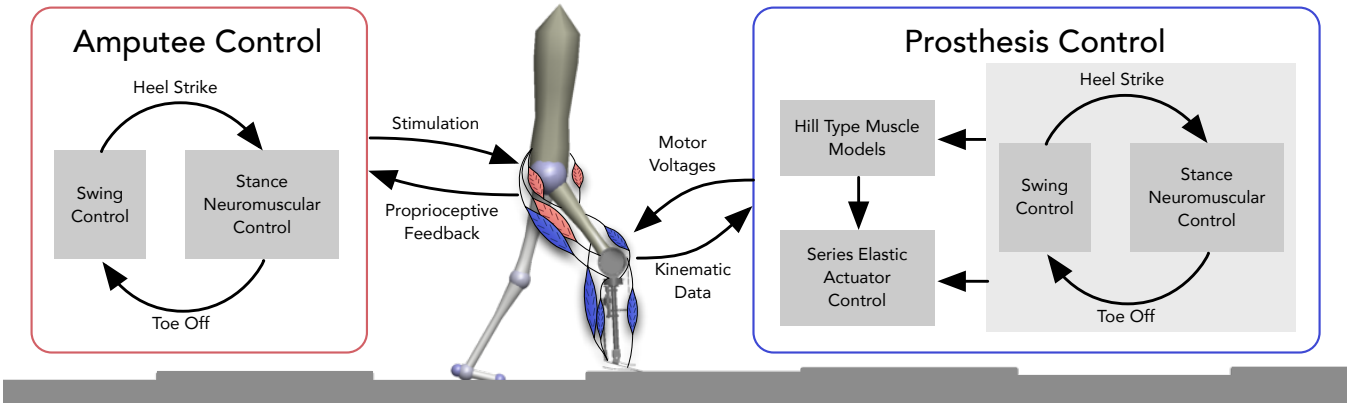


Fig. 2: Overview of amputee and prosthesis controls. During stance, the amputee model is controlled via reflex stimulations of Hill-type muscles. The model has a full complement of muscles on the intact leg and a gluteus, hip flexor, and monoarticular hamstring on the amputated side shown in red. During swing, the control specifies torques that drive the legs to desired landing angles. The prosthesis control features the same swing and stance controllers as the amputee model. The stance control stimulates virtual muscles shown in blue. The torques produced by these muscles, as well as the torques specified by the swing control, are converted to motor voltages by a series elastic actuator controller.

where $l_0$ is the rest leg length, $l$ is the current leg length, and $k^{ext}$ is a proportional gain.

The swing leg controller also specifies a hip torque in the form of a PD-controller on leg angle,

$$\tau_h^{\alpha} = k_p(\alpha_{tgt} - \alpha) - k_d\dot{\alpha}. \tag{8}$$

This hip torque is supplemented by a feed forward term that neutralizes the disturbance caused by coupling during the knee's stop and extend phase (Equation 6).

$$\tau_h = \tau_h^{\alpha} - 2\tau_k^{iii}. \tag{9}$$

The torques produced by the swing controller augment the forces produced by the Hill-type muscles and reflexes during stance. The swing and stance controls for a leg are mixed in proportion to the amount of weight the leg bears.

## III. Amputee Model and Prosthesis Design

### A. Amputee Walking Simulator

We make several modifications to the neuromuscular model to represent the anatomy and physiology of a transfemoral amputee. Viable amputation sites for a transfemoral amputation that allow prosthesis fitting range from 10 cm above the knee to 7 cm below the hip [19]. In this study, we assume a transfemoral amputation 11 cm above the knee and a successful myodesis of the hamstring, in which the muscle is sutured to the distal end of the femur [20]. As shown in Figure 2, the amputation converts the normally biarticular hamstring muscle into a monoarticular muscle that only spans the hip. Furthermore, we halved the maximum isometric force of the hamstring in order to model the muscle atrophy that afflicts many amputees.

### B. Proposed Prosthesis Design

Next, we attach a powered knee-ankle prosthesis to the femoral stump of the amputee model. The prosthesis, shown in Figure 3, is driven by two series elastic actuators, one for the knee and one for the ankle. The knee actuator consists of a brushless servo motor (TQ-Group ILM85-26), a Harmonic Drive gearset (CSF-32-30), and a series composite leaf spring. The ankle actuator consists of another brushless servomotor (TQ-Group ILM85-13), a ballscrew transmission (Nook Industries MBN 8x6 RA V-Thread), and a series composite leaf spring. The ankle joint also contains a parallel spring that can perform conservative work during the gait cycle. We expect this design will achieve peak knee torques of 270 N-m and ankle torques of 160 N-m, peak knee speeds of 12 rad-s$^{-1}$ and ankle speeds of 9 rad-s$^{-1}$, and a prosthetic leg mass of 5 kg with an additional 5 kg carried in a backpack for batteries and motor controllers. These numbers envelop the peak torques and speeds seen during stumble recovery [21], [22].

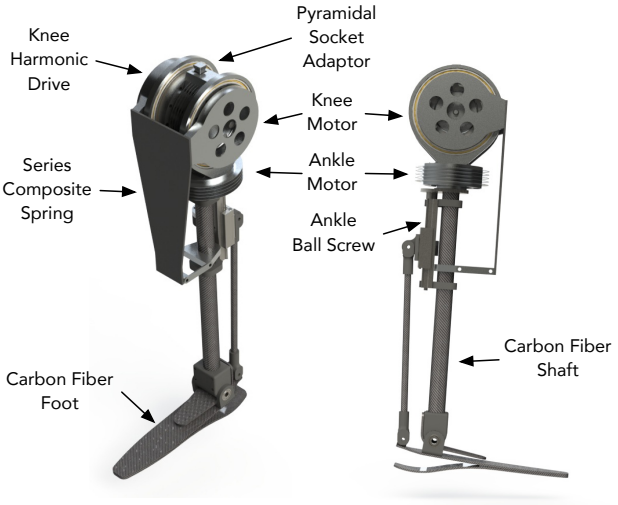


Fig. 3: CAD render of proposed prosthesis design.

### C. Proposed Local Reflex Prosthesis Control

To control the prosthesis, we implement a neuromuscular virtual model controller that simulates five muscles that span the knee and ankle joints: a soleus, gastrocnemius, tibialis anterior, vastus, and biarticular hamstring. These virtual muscles are shown in blue in Figure 2. We stimulate these muscles with the same stance reflexes as used on the intact side. The torques generated by the virtual muscles are then actuated by the prosthesis using a series elastic actuator controller [23].

To calculate the state and stimulation feedbacks of the soleus, gastrocnemius, tibialis anterior, and vastus, we only require joint angle information from the knee and ankle of the prosthesis, which we can obtain via encoders. On the other hand, the virtual biarticular hamstring requires measurement of both the knee and hip joints. We assume that we can obtain hip angle information via an inertial measurement unit (IMU) mounted on the torso of the amputee.

The prosthetic leg control also includes a modified version of the swing leg controller described in section II-B. According to Equation 3, the swing leg control drives the leg towards a target leg angle, $\alpha_{tgt}$, which is a function of the center of mass and stance leg ankle positions. As the prosthesis does not have access to this information, the adaptive leg placement strategy is replaced by a constant target leg angle.

The last change is made to the hip controller, which has a feed forward term based on the knee stopping torque at the end of swing (Equation 9). This feed forward term is not implemented on the amputated side, thereby requiring that feedback torques (Equation 8) handle this disturbance.

Finally, we assume we can obtain the leg angle via an IMU mounted on the prosthesis and that we can calculate the leg length given the knee angle and lengths of the femur and prosthetic shank.

## IV. Evaluation with Simulated Experiments

To evaluate our proposed control, we perform optimizations to find control parameters and then compare the rough ground walking performance of our controller to that of the state-of-the-art impedance controller. In a second test, we compare responses to a simulated tripping event.

### A. Optimization

To obtain natural and robust locomotion we use the covariance matrix adaptation evolution strategy (CMA-ES) [24] in a two step process to optimize the model and control parameters. In the first step, we seek to find a set of parameters that produce a natural gait over flat terrain. We refer to previous work that suggests humans may select gait for energy efficiency [25]. Therefore, we choose to optimize a cost function inspired by the cost of transport of the model,

$$Cost = \frac{W + \int \left(c_1 \tau_{swing}^2 + c_2 \tau_{limit}^2\right) dt}{mgx}, \qquad (10)$$

where $W$ is the muscular energy consumption according to [26], $\tau_{swing}$ is the sum of torques produced by the swing controller, $\tau_{limit}$ is the sum of joint limit torques in the amputee model, $m$ is the mass of the amputee, $g$ is the acceleration due to gravity, and $x$ is the distance travelled in 20 seconds. We initialize the optimization with hand-tuned gains and run simulations to evaluate the cost function.

In a second step, we use the parameters found in step one as the seed for an optimization for walking over rough terrain. We employ the following cost function in this step

$$Cost = -x + c_1 \int \tau_{limit}^2 dt. \qquad (11)$$

To evaluate this cost function we perform walking simulations over five walkways that are flat for the first 10 meters and then feature random steps that increase in severity along the paths. The five sampled walkways are identical across all iterations of the optimization. We use the average cost over the five walkways to compute the final cost for a set of parameters.

### B. Comparison to Impedance Control

We compare our controller to the state-of-the-art impedance prosthesis control [8]–[11]. We found the version presented in [9] produced the best gait on our prosthesis and thus, we implement this controller as a baseline. The impedance control splits the gait cycle into four phases and uses a passive impedance function of the form

$$\tau = -k_1(\theta - \theta_1) - k_2(\theta - \theta_2)^3 - b\dot{\theta} \qquad (12)$$

for each joint in each phase. In this function, $\theta$ is the joint angle, $\theta_1$ and $\theta_2$ are the angle offset positions and $k_1$, $k_2$, and $b$, are the impedance parameters. We optimize this controller's parameters using the procedure described in the previous section.

### C. Rough Ground Locomotion

To compare the robustness of the two controllers, we tested the amputee walking model on eleven 90 meter long walkways featuring random steps with heights ranging from 0 cm (1st walkway) to $\pm$10 cm (11th walkway). Figure 4 shows the distribution of distances achieved by both controllers over forty-five trials at each ground roughness. The two controllers traverse the full distance of the course up to a roughness of $\pm$3 cm. At $\pm$4 centimeters, the performance of the impedance controller begins to fall off and very few samples successfully complete the entire course. In contrast, at this roughness level, most of the reflex controlled prostheses traverse the whole course and over 75% surpass the median performance of the impedance controller. By the 5 centimeter roughness level, most of the impedance function controlled prostheses fall within eighteen meters, whereas several reflex controlled prostheses still manage to negotiate the entire course.

The performance gap between the amputee model and a non-amputee model remains quite large, with the intact model traversing up to $\pm$8 centimeters with a 100% success rate as shown by the blue line in Figure 4. A possible reason for this difference is the constant target leg angle used for

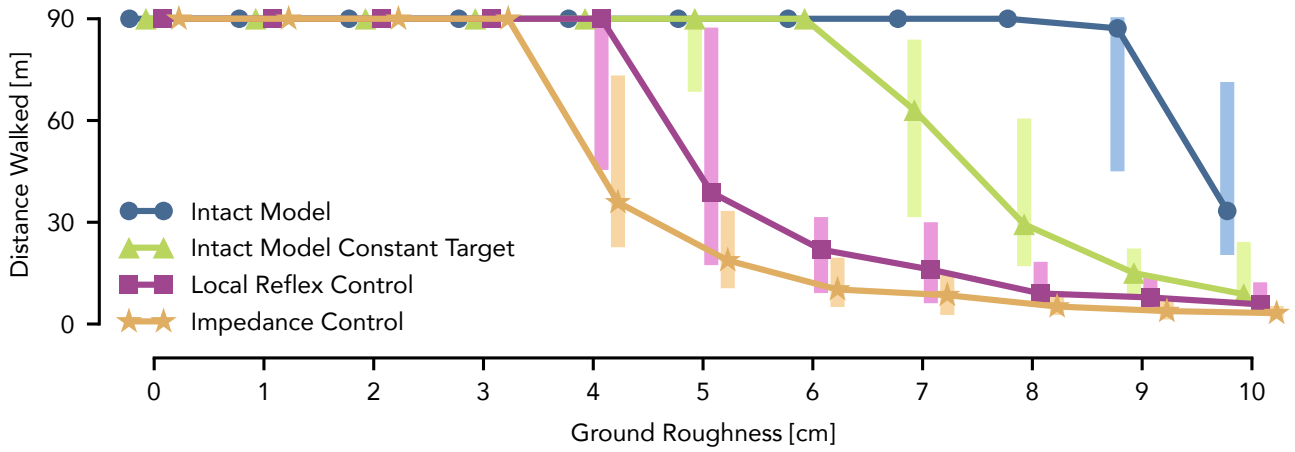


Fig. 4: Distances walked by an intact neuromuscular model, an intact model with a constant target leg angle for one knee, and the amputee model with local reflex and impedance controlled prostheses. Tests are performed on 90 m walkways with random steps drawn from uniform distributions with widths ranging from 0 to $\pm 10$ centimeters. Forty-five walkways are sampled for each roughness level. The trend lines show the median distances walked at each roughness. The bottoms and tops of the boxes mark the $25^{\text{th}}$ and $75^{\text{th}}$ quartiles respectively.

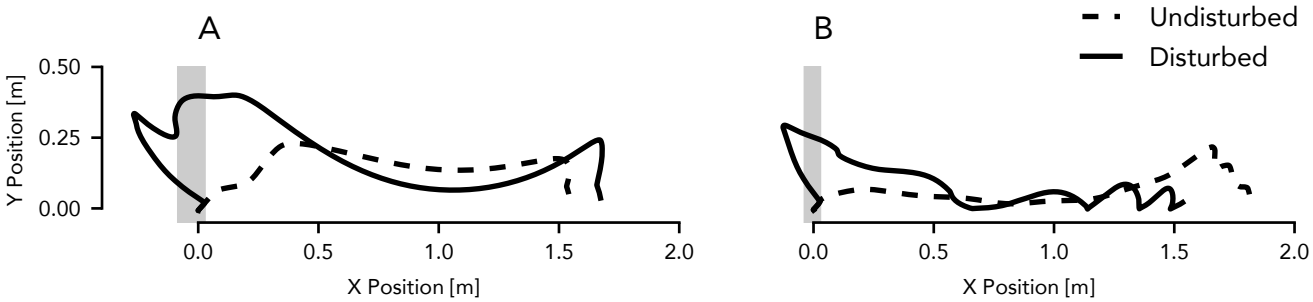


Fig. 5: Prosthetic toe trajectory with reflex control (A) and impedance control (B) during undisturbed gait and when disturbed by a 20 N-s impulse. The impulse is applied as a 2000 N force for 10 ms beginning at 5% of the swing duration. The shaded areas denote the portions of the trajectories along which this impulse acts. The local reflex control effectively responds to the disturbance and maintains a qualitatively similar toe trajectory. In contrast, the impedance controller does not apply appropriate torques resulting in foot scuffing and an eventual fall.

the prosthetic knee control as described in subsection III-C. To explore this possibility, we tested an intact model with this same limitation in one knee. Its performance lies in between that of the reflex controlled prosthesis and the normal intact model. Therefore, the constant target angle used in the prosthesis control is likely responsible for some of the performance gap. Obtaining estimates of the center of mass velocity and stance ankle position should be a focus of future work so this restriction can be lifted. Other sources for the performance difference may be inertial differences between the prosthesis and the healthy leg, the reduced strength of the amputee model, lag in the series elastic actuator torque tracking, and the increased number of parameters in the amputee models, which may reduce the quality of the optimized solutions.

### *D. Simulated Trip Response*

A possible reason why local reflex control may result in more robust locomotion is that it attempts to reproduce the actual human motor control instead of controlling around nominal joint patterns. To investigate this hypothesis, we subjected the amputee model to a simulated tripping event by applying a 2000 N force in the negative-x direction to the prosthetic ankle for 10 ms at the onset of swing. The toe trajectory produced by the reflex controller is shown in Figure 5A. The disturbed trajectory, from mid-swing onwards, is qualitatively similar to the undisturbed trajectory. Consequently, the amputee is able to recover from the stumble and continue walking. The improvement in robustness may be due to the control's feedback loops about global angles, which is important for achieving an appropriate landing leg angle.

In contrast, the impedance control strategy does not attempt to expose underlying control and instead tries to drive the prosthesis around a nominal trajectory corresponding to steady state walking. When perturbed from this nominal trajectory, as is often the case during rough ground walking, these impedance functions may not provide the correct torques to return to the nominal trajectory or recover from the disturbance on subsequent steps. Figure 5B illustrates this effect. When subjected to the impulse, the impedance controller applies the same joint torques as functions of joint angles as in the undisturbed case. As a result, the knee does not extend, the foot scrapes the ground, and the amputee falls, as shown in Figure 1B.

## V. CONCLUSION

Our goal is to build a transfemoral prosthesis with automatic stumble and push recovery that would help prevent falls and encourage amputees to live more active, unfettered lives. In this work, we have shown the potential of reflex control to achieve this goal via simulated amputee walking trials in which our controller outperforms the state-of-the-art impedance controller by walking farther, over rougher terrain and rejecting disturbances with greater ease.

Before advancing to hardware development, we intend to replace the ideal torque implementation of the swing leg controller with a recently developed muscle reflex version [27]. Integrating the muscle reflex swing control into the amputee model and prosthesis control will allow for direct minimization of muscular energy consumption without the penalty terms on swing torques present in Equation 10. This should produce a more natural gait while requiring less hand-tuning of the cost function.

## ACKNOWLEDGMENT

This material is based upon work supported by the National Science Foundation Graduate Research Fellowship under Grant No. 0946825 and the Robotics Institute, Carnegie Mellon University. We thank Carly Sombric for helpful discussions and implementation of the muscle energy models.

## REFERENCES

[1] K. Ziegler-Graham, E. J. MacKenzie, P. L. Ephraim, T. G. Travison, and R. Brookmeyer, "Estimating the prevalence of limb loss in the united states: 2005 to 2050," *Archives of physical medicine and rehabilitation*, vol. 89, no. 3, pp. 422–429, 2008.

[2] W. C. Miller, M. Speechley, and B. Deathe, "The prevalence and risk factors of falling and fear of falling among lower extremity amputees," *Archives of physical medicine and rehabilitation*, vol. 82, no. 8, pp. 1031–1037, 2001.

[3] A. L. Hof, R. M. van Bockel, T. Schoppen, and K. Postema, "Control of lateral balance in walking: experimental findings in normal subjects and above-knee amputees," *Gait posture*, vol. 25, no. 2, pp. 250–258, 2007.

[4] A. Vrieling, H. Van Keeken, T. Schoppen, E. Otten, A. Hof, J. Halbertsma, and K. Postema, "Balance control on a moving platform in unilateral lower limb amputees," *Gait posture*, vol. 28, no. 2, pp. 222–228, 2008.

[5] P. F. Pasquina, P. R. Bryant, M. E. Huang, T. L. Roberts, V. S. Nelson, and K. M. Flood, "Advances in amputee care," *Archives of Physical Medicine and Rehabilitation*, vol. 87, no. 3, Supplement, pp. 34 – 43, 2006.

[6] R. Waters, J. Perry, D. Antonelli, and H. Hislop, "Energy cost of walking of amputees: the influence of level of amputation," *J Bone Joint Surg Am*, vol. 58, no. 1, pp. 42–46, 1976.

[7] M. Bellmann, T. Schmalz, and S. Blumentritt, "Comparative biomechanical analysis of current microprocessor-controlled prosthetic knee joints," *Archives of physical medicine and rehabilitation*, vol. 91, no. 4, pp. 644–652, 2010.

[8] F. Sup, A. Bohara, and M. Goldfarb, "Design and control of a powered knee and ankle prosthesis," in *Robotics and Automation, 2007 IEEE International Conference on*, 2007, pp. 4134–4139.

[9] ——, "Design and control of a powered transfemoral prosthesis," *The International Journal of Robotics Research*, vol. 27, no. 2, pp. 263–273, 2008.

[10] F. Sup, H. A. Varol, J. Mitchell, T. J. Withrow, and M. Goldfarb, "Preliminary evaluations of a self-contained anthropomorphic transfemoral prosthesis," *Mechatronics, IEEE/ASME Transactions on*, vol. 14, no. 6, pp. 667–676, 2009.

[11] F. Sup, H. A. Varol, and M. Goldfarb, "Upslope walking with a powered knee and ankle prosthesis: initial results with an amputee subject," *Neural Systems and Rehabilitation Engineering, IEEE Transactions on*, vol. 19, no. 1, pp. 71–78, 2011.

[12] B. E. Lawson, H. A. Varol, F. Sup, and M. Goldfarb, "Stumble detection and classification for an intelligent transfemoral prosthesis," in *Engineering in Medicine and Biology Society (EMBC), 2010 Annual International Conference of the IEEE*. IEEE, 2010, pp. 511–514.

[13] M. F. Eilenberg, H. Geyer, and H. Herr, "Control of a powered ankle–foot prosthesis based on a neuromuscular model," *Neural Systems and Rehabilitation Engineering, IEEE Transactions on*, vol. 18, no. 2, pp. 164–173, 2010.

[14] H. Geyer and H. Herr, "A muscle-reflex model that encodes principles of legged mechanics produces human walking dynamics and muscle activities," *Neural Systems and Rehabilitation Engineering, IEEE Transactions on*, vol. 18, no. 3, pp. 263–273, 2010.

[15] S. Song, R. Desai, and H. Geyer, "Integration of an adaptive swing control into a neuromuscular human walking model," in *Engineering in Medicine and Biology Society (EMBC), 2013 35th Annual International Conference of the IEEE*, 2013, pp. 4915–4918.

[16] A. Hill, "The heat of shortening and the dynamic constants of muscle," *Proceedings of the Royal Society of London. Series B, Biological Sciences*, vol. 126, no. 843, pp. 136–195, 1938.

[17] K. Yin, K. Loken, and M. van de Panne, "Simbicon: Simple biped locomotion control," in *ACM Transactions on Graphics (TOG)*, vol. 26, no. 3. ACM, 2007, p. 105.

[18] R. Desai and H. Geyer, "Robust swing leg placement under large disturbances," in *Robotics and Biomimetics (ROBIO), 2012 IEEE International Conference on*, 2012, pp. 265–270.

[19] B. J. Brown, C. G. Crone, and C. E. Attinger, "Amputation in the diabetic to maximize function," in *Seminars in Vascular Surgery*, vol. 25, no. 2. Elsevier, 2012, pp. 115–121.

[20] F. Gottschalk, "Transfemoral amputation: biomechanics and surgery," *Clinical orthopaedics and related research*, vol. 361, pp. 15–22, 1999.

[21] M. L. Madigan and E. M. Lloyd, "Age-related differences in peak joint torques during the support phase of single-step recovery from a forward fall," *The Journals of Gerontology Series A: Biological Sciences and Medical Sciences*, vol. 60, no. 7, pp. 910–914, 2005.

[22] M. D. Grabiner, T. J. Koh, T. M. Lundin, and D. W. Jahnigen, "Kinematics of recovery from a stumble," *Journal of gerontology*, vol. 48, no. 3, pp. M97–M102, 1993.

[23] G. Pratt and M. Williamson, "Series elastic actuators," in *Intelligent Robots and Systems 95. 'Human Robot Interaction and Cooperative Robots', Proceedings. 1995 IEEE/RSJ International Conference on*, vol. 1, 1995, pp. 399–406 vol.1.

[24] N. Hansen, "The cma evolution strategy: A comparing review," in *Towards a New Evolutionary Computation*, ser. Studies in Fuzziness and Soft Computing, J. Lozano, P. Larraaga, I. Inza, and E. Bengoetxea, Eds. Springer Berlin Heidelberg, 2006, vol. 192, pp. 75–102.

[25] R. McNeill Alexander, "Energetics and optimization of human walking and running: the 2000 raymond pearl memorial lecture," *American Journal of Human Biology*, vol. 14, no. 5, pp. 641–648, 2002.

[26] B. R. Umberger, K. G. Gerritsen, and P. E. Martin, "A model of human muscle energy expenditure," *Computer methods in biomechanics and biomedical engineering*, vol. 6, no. 2, pp. 99–111, 2003.

[27] R. Desai and H. Geyer, "Muscle-reflex control of robust swing leg placement," in *Robotics and Automation (ICRA), 2013 IEEE International Conference on*, May 2013, pp. 2169–2174.